European Journal of Pharmaceutics and Biopharmaceutics 175 (2022) 1–6

Contents lists available at ScienceDirect

European Journal of Pharmaceutics and Biopharmaceutics

journal homepage: www.elsevier.com/locate/ejpb

# *In vivo* biodistribution of edelfosine-loaded lipid nanoparticles radiolabeled with Technetium-99 m: Comparison of administration routes in mice

Beatriz Lasa-Saracíbar [a], Souhaila H. El Moukhtari [a,d], Theodoros Tsotakos [b], Stavros Xanthopoulos [b], George Loudos [c], Penelope Bouziotis [b,*], Maria J. Blanco-Prieto [a,d,*]

[a] Department of Pharmacy and Pharmaceutical Technology, School of Pharmacy and Nutrition, University of Navarra, Pamplona, Spain
[b] Institute of Nuclear & Radiological Sciences & Technology, Energy & Safety, National Center for Scientific Research "Demokritos", Athens, Greece
[c] BIOEMTECH, 387 Mesogeion Av, 15343 Agia Paraskevi, Athens, Greece
[d] Instituto de Investigación Sanitaria de Navarra (IdiSNA), Pamplona, Spain

ARTICLE INFO

*Keywords:*
Edelfosine
Lipid nanoparticles
Technetium-99*m*
Biodistribution

ABSTRACT

Edelfosine (ET) is a potent antitumor agent but causes severe side effects that have limited its use in clinical practice. For this reason, nanoencapsulation in lipid nanoparticles (LNs) is advantageous as it protects from ET side-effects. Interestingly, previous studies showed the efficacy of LNs containing ET in various types of tumor. In this paper, biodistribution studies of nanoencapsulated ET, administered by three routes (oral, intravenous (IV) and intraperitoneal (IP)), were tested in order to select the optimal route of administration. To do this, ET-LNs were labeled with Technetium-99 m ($^{99m}$Tc) and administered by the oral, IV and IP route in mice. IV administration of the radiolabeled LNs led to fast elimination from the blood circulation and increased accumulation in reticulo-endothelial (RES) organs, while their oral administration could not provide any evidence on their biodistribution since large radiocomplexes were formed in the presence of gastrointestinal fluids. However, when the LNs were administered by the IP route they could access the systemic circulation and provided more constant blood ET-LN levels compared to the IV route. These findings suggest that the IP route can be used to sustain the level of drug in the blood and avoid accumulation in RES organs.

## 1. Introduction

Nanomedicine is a medical and pharmaceutical branch where nanosized materials are used to prevent, treat, or diagnose diseases, with the aim of ameliorating patients' quality of life [1]. Moreover, nanomedicines represent a major class in cancer therapy [2]. Over the last 20 years, nanomedicines have reduced the toxicity associated with anticancer agents while either maintaining or increasing their efficacy [3]. Among them, lipid nanoparticles (LNs) are specially interesting due to their simplicity, high scalability, and safety. LNs are composed of biodegradable lipids with GRAS status and do not necessarily require the use of organic solvents for their fabrication [2]. Inorganic nanoparticles and lipid-based nanomedicines (including LNs and liposomes) represent the vast majority of clinically approved nanoparticles [4]. In fact, as Anselmo and Mitragori mentioned, the first (doxorubicin liposomes) and last (mRNA-1273 vaccine) clinically approved nanomedicines are lipid-based nanoparticles, showing their relevance in the current clinics [4]. The LNs studied here, were originally described in the early 90′s by Müller and collaborators with the idea of manufacturing stable and safe solid lipid nanocarriers that allow for the controlled release of molecules [5]. It should be noted that LNs can be administered by both the i.v. and the oral route which is one their main advantages. Oral lipid nanomedicines are cost-effective, patient friendly and most importantly, able to increase bioavailability and reduce first pass metabolism [6].

Edelfosine (ET) is a synthetic alkyl-lysophospholipid with potent antitumoral activity but unable to reach the clinic due to its gastrointestinal toxicity and hemolytic properties. Although its mechanism of action has not been fully elucidated yet, ET is thought to induce apoptosis specifically in tumor cells. LNs have been widely used to encapsulate antitumor drugs and, among all these formulations, LNs containing ET have shown improved bioavailability and pharmacokinetics profile, high antitumor efficacy, and decreased toxicity in comparison to the free drug [7–9]. ET-LNs have proven *in vitro* and *in vivo* efficacy against several kinds of cancers including both solid and blood tumors [7,10–12]. Despite the effectiveness of ET in some of these studies, as has been mentioned above, LNs provide multiple advantages

* Corresponding authors.
*E-mail addresses:* bouzioti@rrp.demokritos.gr (P. Bouziotis), mjblanco@unav.es (M.J. Blanco-Prieto).

https://doi.org/10.1016/j.ejpb.2022.04.007
Received 14 January 2022; Received in revised form 8 April 2022; Accepted 19 April 2022
Available online 21 April 2022

over the use of ET alone and allow for a more effective and safe therapy [2].

Pharmacokinetic and biodistribution studies in animal models are a mandatory milestone in the development of novel drug delivery systems, as they determine their fate and biological action [13]. Biodistribution studies have been previously established by our group by measuring ET concentration in tissues, but we know that this technique has its own limitations. Indeed, by measuring the amount of ET distributed in tissues, we are not able to measure whether ET reached the organs free or nanoencapsulated. Henceforth, by radiolabeling these LNs we aim to investigate the real biodistribution of LNs containing ET in a sensitive, specific, and quantitative manner.

Radiolabeling of drug-loaded nanoparticles allows for the investigation of their kinetics through *ex vivo* biodistribution and *in vivo* imaging studies. The radiochemist has a large variety of radionuclide in their arsenal, which can be used to investigate the *in vivo* kinetics of a novel nanoconstruct/drug carrier. Noninvasive evaluation of LN biodistribution can be accomplished after their radiolabeling with $^{99m}$Tc, which is one of the radionuclides of choice for short-term assessment of nanomaterial biokinetics, due to certain favorable properties such as low-energy, single gamma-photon emission (140 keV), short half-life ($t_{1/2}$ = 6 h) and availability from affordable $^{99}$Mo/$^{99m}$Tc generators [14–16]. $^{99m}$Tc can be used for chelator-free radiolabelling of various nanostructures, as it associates to various surface groups existing on the nanoparticle's surface [17–20]. The present work hopes to elucidate the *in vivo* distribution profile of ET-LNs after their oral, intravenous (IV) and intraperitoneal (IP) administration in mice. This will be accomplished by the radiolabeling of LNs and determination of their biodistribution after their administration to healthy mice. The obtained results will help us select the most appropriate route of administration for the drug delivery system under evaluation in the present work.

## 2. Materials and methods

### 2.1. Materials

Warning! $^{99m}$Tc is a gamma-emitting radioisotope which presents serious health threats and requires special radioprotective handling to reduce risks associated with its use. Part of the research described herein was conducted at a radiochemical facility which has all the necessary infrastructure, expertise and licenses to conduct radioactivity-associated experiments.

ET was purchased from APOINTECH (Salamanca, Spain). Precirol® ATO 5 was a gift from Gattefossé (France). Tween® 80 was purchased from Roig Pharma (Barcelona, Spain). Chloroform was from Panreac (Madrid, Spain), formic acid 99 % for mass spectroscopy was obtained from Fluka (Barcelona, Spain), and methanol was purchased from Merck (Barcelona, Spain). All solvents employed for the chromatographic analysis were of analytical grade; all other chemicals were of reagent grade and used without further purification. Amicon Ultra-15 10,000 MWCO centrifugal filter devices were purchased from Millipore (Cork, Ireland). $^{99m}$Tc, as Na$^{99m}$TcO$_4$, was eluted from a commercial $^{99}$Mo/$^{99m}$Tc generator (Mallinckrodt Medical B.V.).

### 2.2. Preparation of lipid nanoparticles

LNs were prepared by the hot homogenization method consisting of high shear homogenization and ultrasonication [9]. ET (30 mg) and the lipid (Precirol® ATO 5, ~ 300 mg) were heated 5 °C above the lipid melting point at 70 °C. Then, 10 mL of an an aqueous solution of Tween 80 (2 %), previously heated at the same temperature, was poured onto the lipid phase and the mixture was dispersed and homogenized by a Microson™ ultrasonic cell disruptor (NY, USA) for 1 min with an effective power of 10 W and with an Ultraturrax® (IKA-Werke, Germany) for 1 min at 24 000 rpm. The emulsion was removed from the heat and placed in an ice bath to obtain LN by lipid solidification for at least 15 min. Then, the LN suspension was centrifuged (5000 g for 30 min) and washed twice with distilled water. Afterwards, 150 % (w/w of lipid weight) trehalose was added as cryoprotectant agent to the LN suspension, which was then kept at −80 °C and freeze-dried to obtain a nanoparticulate powder. Particle size and polydispersity index (PDI) were evaluated by photon correlation spectroscopy (PCS) using a Zetasizer Nano (Malvern Instruments, UK). Surface charge was measured using the same Zetasizer Nano equipment combined with laser Doppler velocimetry. For the ET loading determination, the formulation was analyzed by a previously validated ultra-high-performance liquid chromatography tandem mass spectrometry (UHPLC-MS/MS) method [21].

### 2.3. Radiolabeling of lipid nanoparticles

The nanoparticles were radiolabeled with $^{99m}$Tc by the direct labeling method using $SnCl_2$ as the reducing agent. 30 μL of an acidic, aqueous solution containing $SnCl_2$ (10 mg dissolved in 500 μL HCl 37 %, diluted to 10 mL, 1 mg/mL) were added to 100 μL (~300 μCi) pertechnetate eluate ($^{99m}TcO_4^-$). The pH was adjusted to the range of 6–7 with an aqueous solution of $NaHCO_3$ 0.5 M (~22 μL). For the preparation of the radiolabeled sample for IV administration, a 20 μL aliquot containing 30 mg/ml of LNs was added to the reduced $^{99m}$Tc and the mixture was shaken horizontally at RT for 30 min. For the preparation of $^{99m}$Tc-LNs for IP/oral administration, a 50 μL aliquot containing 540 mg of LN/ml was added to the reduced $^{99m}$Tc and the mixture was shaken horizontally at RT for 30 min.

### 2.4. Radiochemical evaluation

Quality control of radiolabeling was performed using acetone and a mixture of pyridine: acetic acid: water (3:5:1.5) as the mobile phases, while ITLC-SA (a layer chromatography medium with salicylic acid) sheets were used as the stationary phase. Using acetone as the mobile phase, free pertechnetate is expected to migrate to the front, while radiolabeled LNs and potentially formed reduced/hydrolyzed $^{99m}$Tc ($^{99m}TcO_2$) are expected to remain at the spot. Using the pyridine: acetic acid: water mixture, all radiolabeled forms are expected to migrate to the front except large radiocolloids, consisting primarily of $^{99m}TcO_2$, which are expected to remain at the spot [17,22].

#### 2.4.1. Labeling stability

Stability of the radiolabeled nanoparticles was assessed in the reaction mixture, in serum and in simulated gastric and intestinal medium. Radioanalysis was performed using acetone and a mixture of pyridine: acetic acid: water (3:5:1.5) as the mobile phases and ITLC-SA sheets as the stationary phase, as described above.

#### 2.4.2. Stability in serum

For the serum study, 20 μL of the radiolabeled-LNs were challenged against 180 μL of serum at 37 °C for 1, 2 and 4 h. Aliquots were taken from the mixture and analyzed by ITLC, as described above.

#### 2.4.3. Stability in gastric and intestinal media

Stability in gastric and intestinal medium was assessed by incubating 50 μL of radiolabeled-LNs with 450 μL of simulated gastric medium (0.1 M HCl in PBS; pH = 1.5) or intestinal medium (0.05 M Potassium phosphate monobasic in water; pH = 6.8) at 37 °C for 1, 2 and 4 h. Aliquots were taken from the mixtures and analyzed by ITLC, as demonstrated above.

### 2.5. Imaging and biodistribution studies

Female normal Swiss mice (average weight of 20 g) of the same colony and age (approximately 6 weeks) were purchased from the Breeding Facilities of the Institute of Biosciences and Applications

'Demokritos'. *In vivo* studies were performed in compliance with European legislation, while Greek authorities approved all animal protocols. The experimental facility of the NCSR "Demokritos" is registered according to the Greek Presidential Decree 56/2013 (Reg Number El 25 BIO 022) in accordance to the European Directive 2010/63 which is harmonized with national legislation, on the protection of animals used for scientific purposes.

All imaging studies were performed using a dedicated 2D scintigraphic camera (BIOEMTECH, GR), which has 1.5 mm spatial resolution and allows the entire mouse to fit in the field of view, thus providing fast whole-body frames. Then regions of interest (ROIs) were drawn around the organs of interest and the number of counts in each ROI divided by the number of counts in the entire mouse was calculated to provide the percentage of radioactivity per organ, at each time point.

#### 2.5.1. Oral administration

Mice received one single oral dose of [$^{99m}$Tc]Tc-ET-LN (200 μL; 30 mg ET-LN/Kg; ~ 300 μCi) or of free pertechnetate (~300 μCi). The radiotracer was administered orally via a plastic gavage microapparatus. Afterwards, SPECT images were captured at different time points after administration (1.5, 3 and 5.5 h post-administration). The mice were fixed on an animal fixing tray board and imaging was performed.

#### 2.5.2. Intravenous administration (IV)/intraperitoneal injection (IP)

Mice received one single IV dose of [$^{99m}$Tc]Tc-ET-LN (100 μL; 30 mg ET-LN/Kg; ~300 μCi). A second cohort of mice received a single IP injection of [$^{99m}$Tc]Tc-ET-LN (200 μL; 30 mg ET-LN/Kg; ~300 μCi). Afterwards, SPECT images were captured at different time points after administration (1-, 4- and 24-hours post-administration). Mice were fixed on an animal fixing tray board and imaging was performed.

For the biodistribution studies via the IV mode of administration, mice (n = 3; 3 groups) received one single IV dose of [$^{99m}$Tc]Tc-ET-LN (100 μL; 30 mg ET-LN/Kg), while for i.p. administration mice received one single IP dose of radiolabeled LNs (200 μL; 30 mg ET-LN/Kg; ~ 300 μCi). Then, the animals were euthanized at 4, 24 and 48 h post-administration, and their major organs and tissues were removed, together with samples of muscles, and were weighed and counted in an automated well-typed gamma scintillation counter Cobra II (Canberra, Packard, Downers Grove, IL, USA) calibrated for $^{99m}$Tc. All measurements were corrected for background and radioactive decay. Radioactivity was interpreted as percentage of injected dose (% ID) per gram of organ/tissue, using an appropriate standard. The stomach and intestines were not emptied before the measurements.

## 3. Results and discussion

### 3.1. Lipid nanoparticles characterization

ET-LNs were prepared by the hot homogenization method consisting of high shear homogenization and ultrasonication [9]. This technique yielded LNs with a size of 128 ± 10 nm and negative surface charge (−28 ± 1 mV). The PDI value obtained was 0.23 ± 0.02 indicating a homogeneous distribution of particles. ET-LN loading was 23 ± 2 μg ET/mg.

### 3.2. Radiolabeling of lipid nanoparticles

The chemical reactivity of $^{99m}$Tc, when eluted from a $^{99}$Mo/$^{99m}$Tc generator as $^{99m}TcO_4^-$, is negligible. This is the reason why $^{99m}TcO_4^-$ is reduced to lower oxidation states with reducing agents such as stannous chloride ($SnCl_2$). Direct labeling of nanostructures with reduced $^{99m}$Tc relies on the interaction between the Tc(V) reduced ions and deprotonated hydroxyl or carboxyl groups present on the surface of the nanostructure [23,24]. The LNs investigated in this study were prepared by using the lipid Precirol® ATO 5, which is composed of palmitic (C16) and stearic (C18) acids containing both hydroxyl and carboxyl groups. At a pH of around 7, which is the pH of our solution during radiolabeling, the hydroxyl and carboxyl groups may be deprotonated, thus the Tc(V) ions can interact with them and provide stable radiolabeling of the LNs. ET-LNs were radiolabeled with $^{99m}$Tc yielding high labeling efficiency (>97 %) and with minimal amounts of pertechnetate and/or radiocolloids formed during the direct labeling procedure. Stability in the reaction mixture after 2.5 h of preparation was evaluated. Results showed that the sample remained intact with only 3.0 percent of colloid formation, up to 24 h post-labeling. These results confirm the feasibility of using $^{99m}$Tc to effectively label LNs as has been previously stated by other authors [25].

### 3.3. Stability of radiolabeling in media

#### 3.3.1. Serum

The serum stability study showed that $^{99m}$Tc was not dissociated and no re-oxidation to pertechnetate took place after 4 h of incubation with serum. However, stability studies showed that larger radiocomplexes are formed as shown by the pyridine: acetic acid: water mixture quality control. This might be due to the interaction with serum proteins. After 30 min of incubation, only 7.8 % of the radiolabeled LNs remained in the reaction mixture. This percentage was maintained after up to 4 h of incubation with serum. These results might promote higher uptake by reticulo-endothelial system (RES) organs due to a larger nanoparticle size [26].

#### 3.3.2. Gastric medium and intestinal medium

In gastric medium, $^{99m}$Tc was not dissociated; no reoxidation to pertechnetate took place after 4 h of incubation with gastric medium. Nevertheless, larger radiocomplexes are formed as shown by the pyridine: acetic acid: water mixture quality control. After 1 h of incubation only 12.6 % of the radiolabeled LNs remained intact. This percentage was lower after 4 h (7.3 %) of incubation. The formation of large radiocomplexes might influence oral absorption of the complexes because it is believed that nanoparticles smaller than 300 nm are better absorbed by the oral route [26].

Concerning the intestinal medium, $^{99m}$Tc was not dissociated. However, as observed for both the serum and gastric media, larger radiocomplexes were formed, as shown by the pyridine: acetic acid: water mixture quality control. After 1 h of incubation only 9.5 % of the radiolabeled LNs remained intact. This percentage was similar after 4 h of incubation. The formation of larger radiocomplexes in gastric and intestinal media might be caused by the coagulation of labeled LNs in these media.

### 3.4. Oral administration of Na[$^{99m}$Tc]$TcO_4$ / [$^{99m}$Tc]Tc-ET-LNs

*In vivo* imaging results showed that free pertechnetate Na[$^{99m}$Tc]$TcO_4$ was absorbed in the stomach after its oral administration, and was concentrated in thyroid area, lungs, stomach and bladder (Fig. 1: A–B). In contrast, [$^{99m}$Tc]Tc-ET-LNs were not distributed through the body after oral administration (Fig. 1:C–D). In fact, after 7 h post-administration, the radioactive signal was still concentrated in the intestines and stomach indicating that radiolabeled ET-LNs were not absorbed.

These results do not correlate with previous biodistribution results that show oral ET absorption when it is encapsulated into LNs [8]. Nevertheless, the observed gastrointestinal accumulation of radiolabeled-LNs might be due to large radio-complexes formation in acid media (as witnessed by the *in vitro* stability test). As intestinal absorption requires nanoparticles sizes below ~ 300 nm, radio-complexes would not be absorbed and, therefore, accumulate in the gastrointestinal tract. Orally administered radiolabelled LNs go through many physicochemical changes imposed by the gastrointestinal environment. Thus, their stability must be maintained over a long period of time in order to

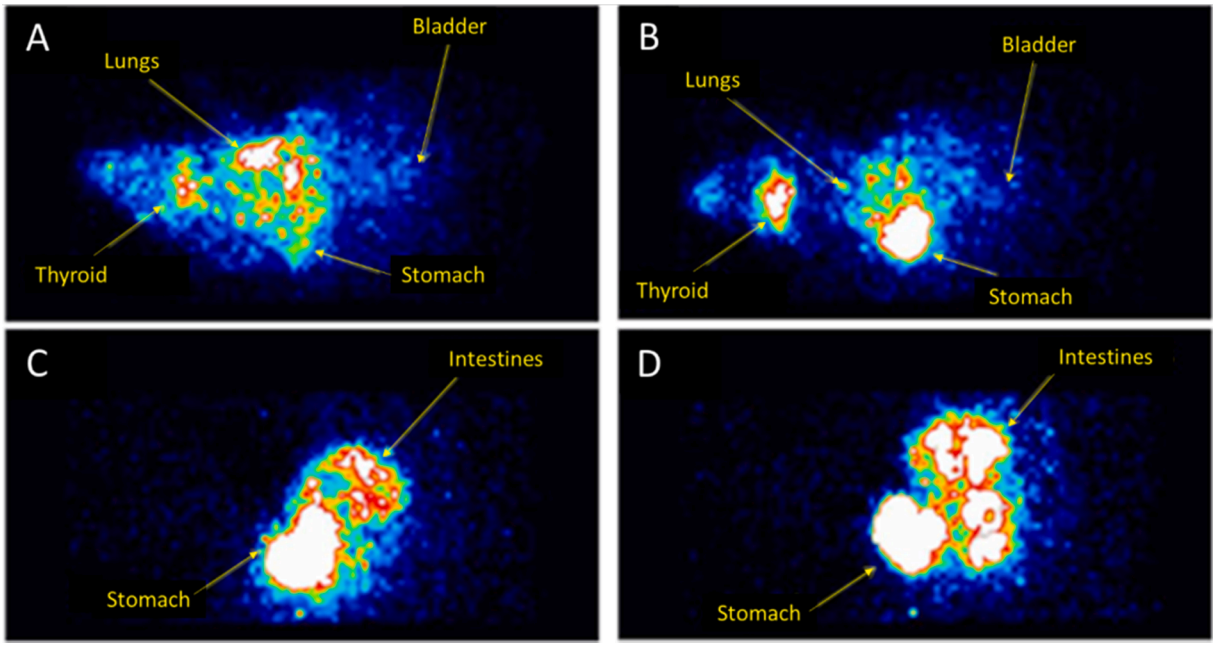


**Fig. 1.** A-B: Static 2-minute images of mice after oral administration of $Na^{99m}TcO_4$ (~300 μCi) 12 min. post administration (A) and 190 min. post-administration (B). C-D: Static 2-minute images of mice after oral administration of $^{99m}$Tc-ET-LN (~300 μCi) 145 min. post administration (C) and 181 min. post-administration (D).

reach the intestinal area of absorption. These physiological changes may have played a role in the low transport observed here.

### 3.5. *Intravenous administration of [$^{99m}$Tc]Tc-ET-LNs.*

Results of biodistribution after IV administration are consistent with the physicochemical characteristics of LNs. Fig. 2 and Fig. 4 show that $^{99m}$Tc-ET-LNs were mainly accumulated in liver, lungs, spleen and kidneys/bladder.

RES clearance is associated with nanoparticles with sizes>200 nm [13]; ET-LNs have a size around 120 nm and thus, large radiocomplexes might be uptaken by the kupffer cells in lymphatic organs such as the spleen and liver. The splenic uptake of radiolabeled ET-LNs was high initially (22.13 % ID at 3 h) but decreased with time, whereas % ID in liver and lungs was maintained or even increased after 24 and 48 h. Besides, very low uptake by the thyroid and stomach indicates that $^{99m}$Tc remained associated to the nanoparticles, as free $^{99m}$Tc accumulates in these organs [27].

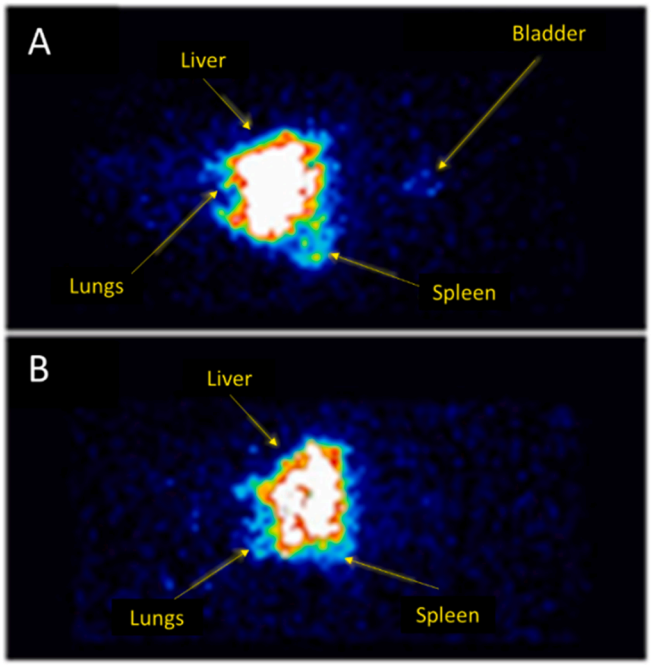


**Fig. 2.** Static 2-minute images of mice after intravenous administration of radiolabeled-LNs (~300 μCi) 10 min. (A) and 24 h (B) post-administration.

Previous drug biodistribution studies in mice showed that free ET is mostly distributed to the lungs, spleen, intestine, liver, and kidneys [28]. Moreover, we know that the gastrointestinal toxicity of ET is strongly correlated to its important uptake into the guts. Table S1 clearly shows that nanoencapsulated ET is poorly distributed to the intestines, which converges with our previous toxicity studies in mice [29].

Estella et al. [8] not only described a similar pattern of distribution but also found an ET-LN accumulation in intestine and kidneys. They explained these accumulations in elimination organs as a result of euthanizing mice 7 days post-administration. As our experiments lasted only for 48 h, due to $^{99m}$Tc half-life, these two studies are not entirely comparable. It was also stated that ET-LN preferentially distributed ET to the brain. However, the present results showed that ET-LNs were preferentially distributed towards the liver, spleen, and lungs but not necessarily to the brain [8]. In these previous biodistribution studies, the location of LNs was not assessed as ET was directly extracted from brain tissue and drug concentration was quantified by UHPLC-MS/MS.

### 3.6. *Intraperitoneal administration of [$^{99m}$Tc]Tc-ET-LNs*

In this case, [$^{99m}$Tc]Tc-ET-LNs were more widely distributed in comparison to IV administration. The radioactive signal was prominent in the stomach, pancreas, intestines, spleen and bladder/kidneys (Figs. 3 and 4). The signal in these organs was almost null at 24 and 48 h post administration, with the exception of the kidneys where the signal was maintained for 48 h. In view of these results, we can conclude that biodistribution of [$^{99m}$Tc]Tc-ET-LNs after IP route differs from the IV route. In general, after IP administration, [$^{99m}$Tc]Tc-ET-LNs are more widely distributed throughout the different organs, avoiding the high accumulation of nanoparticles in liver, lungs and spleen observed after IV administration. These data are in agreement with previous studies regarding $^{99m}$Tc-labeled LN biodistribution after IP and IV injection

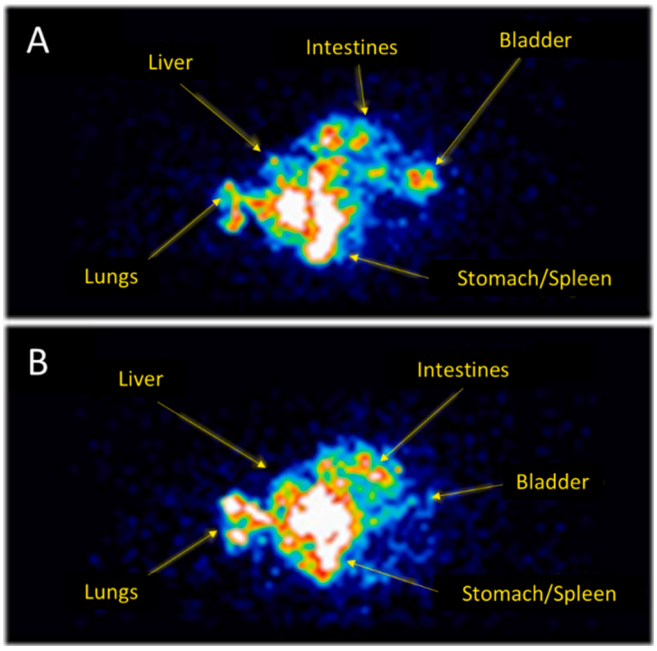


**Fig. 3.** Static 2-minute images of mice after intraperitoneal administration of radiolabeled-LNs (~300 μCi) 120 min. (A) and 284 min. (B) post-administration.

[25]. The accumulated radioactivity in the intestines and stomach might be explained by the direct delivery of the radiolabeled nanoparticles in the peritoneum.

Results of biodistribution after IP administration showed that the total measured radioactivity in the organs/tissues was lower than after IV administration (Fig. 4). Since the initial amount of radioactivity administered in both routes was the same, this lower amount of total radioactivity might be explained by a faster elimination of the $^{99m}$Tc or by an accumulation of [$^{99m}$Tc]Tc-ET-LNs in organs/tissues different from those that were analyzed in the study. Radioactive signal in kidneys was maintained after 24 and 48 h, suggesting sustained elimination of labeled ET-LNs, and was lower after IP administration than after IV administration; thus, faster elimination of labeled ET-LNs after IP administration does not seem to be a likely phenomenon. Therefore, the remaining radioactivity might be located in other organs/tissues such as peritoneal adipose tissue or lymph nodes (radioactivity in these tissues was not measured). In this regard, previous studies [25] refer to biphasic absorption of LNs labeled with $^{99m}$Tc in blood after IP administration due to an initial faster distribution followed by a slow disposition from the peritoneum. This pattern was also observed in this study: blood concentration of $^{99m}$Tc decreased within time after IV administration whereas it was constant after IP administration. These blood and kidney results might support the hypothesis of a depot compartment from which labeled ET-LNs are released to the blood in a sustained manner. Our results support that IP administration allows large complexes such as LNs to access the systemic circulation intact as mentioned by Al Shoyaib et al. [30]. Considering these results, the IP route seems to be an adequate route for the administration of ET-LNs in mice. This might provide lower accumulation of the LNs in RES organs and more constant blood ET-LNs levels.

## 4. Conclusions

ET-LNs were successfully radiolabeled (>97%) with minimal amounts of pertechnetate and/or radiocolloids formed. In addition, *in vitro* studies in various media showed that $^{99m}$Tc was not dissociated from the LNs. No reoxidation to pertechnetate took place after 4 h of incubation with serum, gastric or intestinal media, but large radiocomplexes were formed after incubation with all the different media. This could be the reason for the non-absorption of radiolabeled ET-LNs given orally. IV administration led to swift biodistribution of the labeled ET-LNs with major accumulation of the nanosystems in RES organs such as liver, spleen and lungs. In contrast, the IP route of administration led to very slow biodistribution, while accumulation of the LNs in the RES organs was avoided. The lower radioactive signal in comparison to IV administration suggested accumulation of the [$^{99m}$Tc]Tc-ET-LNs in tissues other than those analyzed in the study. In fact, the sustained radioactive signal in blood and kidneys suggests biphasic absorption of the radiolabeled ET-LNs, which in turn might provide controlled release of the drug over time. In summary, the present study shows that *in vivo*

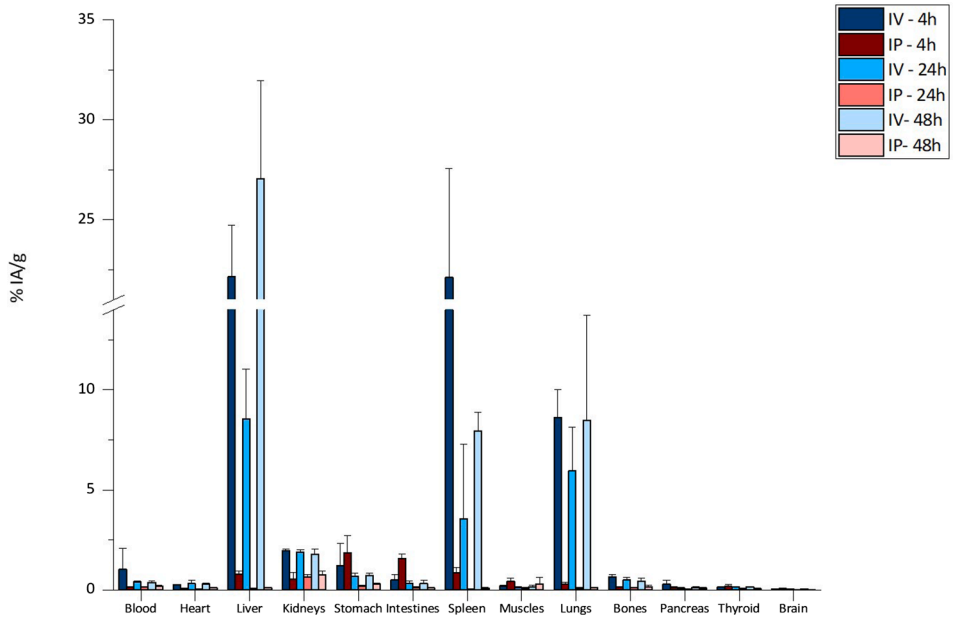


**Fig. 4.** Biodistribution of radiolabeled-LNs in mice after intravenous (IV) and intraperitoneal (IP) administration. The animals were intravenously (IV) or intraperitoneally (IP) administered with $^{99m}$Tc-ET-LN and were sacrificed at 4 h, 24 and 48 h post-injection. Radioactivity was measured in each organ and expressed as percent of injected dose per g of organ/tissue. Each value is the mean ± SD of 3 mice.

tracking of LNs with radiolabeling techniques could provide valuable information on the biodistribution of drug-loaded lipid nanocarriers after their administration *via* different routes.

## Declaration of Competing Interest

The authors declare that they have no known competing financial interests or personal relationships that could have appeared to influence the work reported in this paper.

## Acknowledgments

This work was carried out in the framework of the COST Action TD1004. Financial support from Caja Navarra Foundation, University of Navarra (FUN), the Government of Navarra, Department of Health (ref: 63/09, "Ortiz de Landázuri" fellowship) and the Spanish Ministry of Science and Innovation (SAF2010-15547) are acknowledged. B. Lasa-Saracibar is supported by the research grant from "Asociación de Amigos de la Universidad de Navarra".

## Appendix A. Supplementary material

Supplementary data to this article can be found online at https://doi.org/10.1016/j.ejpb.2022.04.007.

## References

[1] P. Boisseau, B. Loubaton, Nanomedicine, nanotechnology in medicine, Comptes Rendus Phys. 12 (2011) 620–636, https://doi.org/10.1016/j.crhy.2011.06.001.
[2] B. Lasa-Saracibar, A. Estella-Hermoso de Mendoza, M. Guada, C. Dios-Vieitez, M. J. Blanco-Prieto, Lipid nanoparticles for cancer therapy: state of the art and future prospects, Expert Opin. Drug Deliv. 9 (10) (2012) 1245–1261, https://doi.org/10.1517/17425247.2012.717928.
[3] J. Shi, P.W. Kantoff, R. Wooster, O.C. Farokhzad, Cancer nanomedicine: Progress, challenges and opportunities, Nat. Rev. Cancer. 17 (1) (2017) 20–37, https://doi.org/10.1038/nrc.2016.108.
[4] A.C. Anselmo, S. Mitragotri, Nanoparticles in the clinic: An update post COVID-19 vaccines, Bioeng. Transl. Med. 6 (2021), e10246, https://doi.org/10.1002/btm2.10246.
[5] R.H. Müller, K. Mäder, S. Gohla, Solid lipid nanoparticles (SLN) for controlled drug delivery – a review of the state of the art, Eur. J. Pharm. Biopharm. 50 (2000) 161–177, https://doi.org/10.1016/S0939-6411(00)00087-4.
[6] S.H. El Moukhtari, C. Rodríguez-Nogales, M.J. Blanco-Prieto, Oral lipid nanomedicines: Current status and future perspectives in cancer treatment, Adv. Drug Deliv. Rev. 173 (2021) 238–251, https://doi.org/10.1016/j.addr.2021.03.004.
[7] A. Estella-Hermoso de Mendoza, M.A. Campanero, H. Lana, J.A. Villa-Pulgarin, J. de la Iglesia-Vicente, F. Mollinedo, M.J. Blanco-Prieto, Complete inhibition of extranodal dissemination of lymphoma by edelfosine-loaded lipid nanoparticles, Nanomedicine. 7 (5) (2012) 679–690, https://doi.org/10.2217/nnm.11.134.
[8] A. Estella-Hermoso de Mendoza, V. Préat, F. Mollinedo, M.J. Blanco-Prieto, In vitro and in vivo efficacy of edelfosine-loaded lipid nanoparticles against glioma, J. Control. Release. 156 (3) (2011) 421–426, https://doi.org/10.1016/j.jconrel.2011.07.030.
[9] M.Á. Aznar, B. Lasa-Saracíbar, A. Estella-Hermoso de Mendoza, M.J. Blanco-Prieto, Efficacy of edelfosine lipid nanoparticles in breast cancer cells, Int. J. Pharm. 454 (2) (2013) 720–726, https://doi.org/10.1016/j.ijpharm.2013.04.068.
[10] B. Lasa-Saracíbar, A. Estella-Hermoso de Mendoza, F. Mollinedo, M.D. Odero, M. J. Blanco-Príeto, Edelfosine lipid nanosystems overcome drug resistance in leukemic cell lines, Cancer Lett. 334 (2) (2013) 302–310, https://doi.org/10.1016/j.canlet.2013.01.018.
[11] F. Mollinedo, J. de la Iglesia-Vicente, C. Gajate, A. Estella-Hermoso de Mendoza, J. A. Villa-Pulgarin, M.A. Campanero, M.J. Blanco-Prieto, Lipid raft-targeted therapy in multiple myeloma, Oncogene. 29 (26) (2010) 3748–3757, https://doi.org/10.1038/onc.2010.131.
[12] F. Mollinedo, J. de la Iglesia-Vicente, C. Gajate, A.-H. de Mendoza, J.A. Villa-Pulgarin, M. de Frias, G. Roué, J. Gil, D. Colomer, M.A. Campanero, M.J. Blanco-Prieto, In vitro and In vivo Selective Antitumor Activity of Edelfosine against Mantle Cell Lymphoma and Chronic Lymphocytic Leukemia Involving Lipid Rafts, Clin Cancer Res 16 (7) (2010) 2046–2054.
[13] F.H. Zakarial Ansar, S.Y. Latifah, W.H.B. Wan Kamal, K.C. Khong, Y. Ng, J. N. Foong, B. Gopalsamy, W.K. Ng, C.W. How, Y.S. Ong, R. Abdullah, M.Y. Aziz, Pharmacokinetics and Biodistribution of Thymoquinone-loaded Nanostructured Lipid Carrier After Oral and Intravenous Administration into Rats, Int. J. Nanomedicine. 15 (2020) 7703–7717, https://doi.org/10.2147/IJN.S262395.
[14] D. Psimadas, P. Bouziotis, P. Georgoulias, V. Valotassiou, T. Tsotakos, G. Loudos, Radiolabeling approaches of nanoparticles with 99mTc, Contrast Media Mol. Imaging. 8 (2013) 333–339, https://doi.org/10.1002/cmmi.1530.
[15] E.A. Fragogeorgi, I.N. Savina, T. Tsotakos, E. Efthimiadou, S. Xanthopoulos, L. Palamaris, D. Psimadas, P. Bouziotis, G. Kordas, S. Mikhalovsky, M. Alavijeh, G. Loudos, Comparative in vitro stability and scintigraphic imaging for trafficking and tumor targeting of a directly and a novel 99mTc(I)(CO)3 labeled liposome, Int. J. Pharm. 465 (2014) 333–346, https://doi.org/10.1016/j.ijpharm.2014.01.042.
[16] C. Tsoukalas, D. Psimadas, G.A. Kastis, V. Koutoulidis, A.L. Harris, M. Paravatou-Petsotas, M. Karageorgou, L.R. Furenlid, L.A. Moulopoulos, D. Stamopoulos, P. Bouziotis, A Novel Metal-Based Imaging Probe for Targeted Dual-Modality SPECT/MR Imaging of Angiogenesis, Front. Chem. 6 (2018) 224, https://doi.org/10.3389/fchem.2018.00224.
[17] D. Psimadas, G. Baldi, C. Ravagli, P. Bouziotis, S. Xanthopoulos, M.C. Franchini, P. Georgoulias, G. Loudos, Preliminary evaluation of a 99mTc labeled hybrid nanoparticle bearing a cobalt ferrite core: In vivo biodistribution, J. Biomed. Nanotechnol. 8 (2012) 575–585, https://doi.org/10.1166/jbn.2012.1412.
[18] E. Orocio-Rodríguez, G. Ferro-Flores, C.L. Santos-Cuevas, F.d.M. Ramírez, B. E. Ocampo-García, E. Azorín-Vega, F.M. Sánchez-García, Two novel nanosized radiolabeled analogues of somatostatin for neuroendocrine tumor imaging, J. Nanosci. Nanotechnol. 15 (6) (2015) 4159–4169, https://doi.org/10.1166/jnn.2015.9620.
[19] S.M. Ghoreishi, A. Khalaj, O. Sabzevari, L. Badrzadeh, P. Mohammadzadeh, S. S. Mousavi Motlagh, A. Bitarafan-Rajabi, M., Shafiee Ardestani, Technetium-99m chelator-free radiolabeling of specific glutamine tumor imaging nanoprobe: in vitro and in vivo evaluations, Int. J. Nanomedicine. 13 (2018) 4671–4683, https://doi.org/10.2147/IJN.S157426.
[20] M.S. Ardestani, A. Bitarafan-Rajabi, P. Mohammadzadeh, S. Mortazavi-Derazkola, O. Sabzevari, A.D. Azar, S. Kazemi, S.R. Hosseini, S.M. Ghoreishi, Synthesis and characterization of novel 99mTc-DGC nano-complexes for improvement of heart diagnostic, Bioorg. Chem. 96 (2020), 103572, https://doi.org/10.1016/j.bioorg.2020.103572.
[21] A. Estella-Hermoso de Mendoza, M.A. Campanero, F. Mollinedo, M.J. Blanco-Príeto, Comparative study of A HPLC–MS assay versus an UHPLC–MS/MS for anti-tumoral alkyl lysophospholipid edelfosine determination in both biological samples and in lipid nanoparticulate systems, J. Chromatogr. B. 877 (2009) 4035–4041, https://doi.org/10.1016/j.jchromb.2009.10.020.
[22] M. Snehalatha, K. Venugopal, R.N. Saha, A.K. Babbar, R.K. Sharma, Etoposide Loaded PLGA and PCL Nanoparticles II: Biodistribution and Pharmacokinetics after Radiolabeling with Tc-99m, Drug Deliv. 15 (5) (2008) 277–287, https://doi.org/10.1080/10717540802006500.
[23] J. Pellico, P.J. Gawne, R.T.M. de Rosales, Radiolabelling of nanomaterials for medical imaging and therapy, Chem. Soc. Rev. 50 (5) (2021) 3355–3423, https://doi.org/10.1039/D0CS00384K.
[24] M. Das, S.R. Datir, R.P. Singh, S. Jain, Augmented Anticancer Activity of a Targeted, Intracellularly Activatable, Theranostic Nanomedicine Based on Fluorescent and Radiolabeled, Methotrexate-Folic Acid-Multiwalled Carbon Nanotube Conjugate, Mol. Pharm. 10 (7) (2013) 2543–2557, https://doi.org/10.1021/mp300701e.
[25] L. Harivardhan Reddy, R.K. Sharma, K. Chuttani, A.K. Mishra, R.S.R. Murthy, Influence of administration route on tumor uptake and biodistribution of etoposide loaded solid lipid nanoparticles in Dalton's lymphoma tumor bearing mice, J. Control. Release. 105 (3) (2005) 185–198, https://doi.org/10.1016/j.jconrel.2005.02.028.
[26] R. Agarwal, K. Roy, Intracellular delivery of polymeric nanocarriers: a matter of size, shape, charge, elasticity and surface composition, Ther. Deliv. 4 (6) (2013) 705–723, https://doi.org/10.4155/tde.13.37.
[27] A. Beloqui, M.N. Solins, A.R. Gascn, A. del Pozo-Rodrguez, A. des Rieux, V. Prat, Mechanism of transport of saquinavir-loaded nanostructured lipid carriers across the intestinal barrier, J. Control. Release. 166 (2) (2013) 115–123.
[28] A.-H. de Mendoza, M.A. Campanero, J. de la Iglesia-Vicente, C. Gajate, F. Mollinedo, M.J. Blanco-Prieto, Antitumor Alkyl Ether Lipid Edelfosine: Tissue Distribution and Pharmacokinetic Behavior in Healthy and Tumor-Bearing Immunosuppressed Mice, Clin. Cancer Res. 15 (3) (2009) 858–864, https://doi.org/10.1158/1078-0432.CCR-08-1654.
[29] B. Lasa-Saracíbar, M.Á. Aznar, H. Lana, I. Aizpún, A.G. Gil, M.J. Blanco-Prieto, Lipid nanoparticles protect from edelfosine toxicity in vivo, Int. J. Pharm. 474 (1-2) (2014) 1–5, https://doi.org/10.1016/j.ijpharm.2014.07.053.
[30] A. Al Shoyaib, S.R. Archie, V.T. Karamyan, Intraperitoneal Route of Drug Administration: Should it Be Used in Experimental Animal Studies? Pharm. Res. 37 (2019) 12, https://doi.org/10.1007/s11095-019-2745-x.